6-20-2018

Laboratory evaluation on performance of compound-modified asphalt for rock asphalt/styrene–butadiene rubber (SBR) and rock asphalt/nano-CaCO3

Songtao Lv
Michigan Technological University

Shuangshuang Wang
Changsha University of Science & Technology

Tong Guo
XIANDAI TOUZI Co., Ltd

Chengdong Xia
Changsha University of Science & Technology

Jianglong Li
Changsha University of Science & Technology

See next page for additional authors

Recommended Citation

Lv, S., Wang, S., Guo, T., Xia, C., Li, J., & Hou, G. (2018). Laboratory evaluation on performance of compound-modified asphalt for rock asphalt/styrene–butadiene rubber (SBR) and rock asphalt/nano-CaCO3. *Applied Sciences, 8*(6), 1009. http://doi.org/10.3390/app8061009
Retrieved from: https://digitalcommons.mtu.edu/michigantech-p/1915

Authors

Songtao Lv, Shuangshuang Wang, Tong Guo, Chengdong Xia, Jianglong Li, and Gui Hou

applied sciences

MDPI

Article

Laboratory Evaluation on Performance of Compound-Modified Asphalt for Rock Asphalt/Styrene–Butadiene Rubber (SBR) and Rock Asphalt/Nano-$CaCO_3$

Songtao Lv [1,2], Shuangshuang Wang [1], Tong Guo [3], Chengdong Xia [1,*], Jianglong Li [1] and Gui Hou [4]

1 National Engineering Laboratory of Highway Maintenance Technology, Changsha University of Science & Technology, Changsha 410004, China; lst@csust.edu.cn (S.L.); wsscsust@126.com (S.W.); ljl1530@126.com (J.L.)
2 Department of Civil and Environmental Engineering, Michigan Technological University, Houghton, MI 49931, USA
3 XIANDAI TOUZI Co., Ltd., Changsha 410004, China; 18569412272@163.com
4 Inner Mongolia Communications Construction Engineering Quality Supervision Bureau, Hohhot 010051, China; hhhthougui@163.com
* Correspondence: xiachengdong@stu.csust.edu.cn

Received: 11 May 2018; Accepted: 18 June 2018; Published: 20 June 2018

check for updates

Abstract: As a natural modifier of asphalt, rock asphalt has been widely used to improve its thermal stability and aging resistance. However, the thermal cracking resistance of asphalt modified by rock asphalt is unsatisfactory. In order to improve the thermal cracking resistance in low temperature, two kinds of modifiers—styrene–butadiene rubber (SBR) and nano-$CaCO_3$—were selected as the compound modifiers, and then implemented to improve the low-temperature performance of the binder. Then, compound asphalt modified by Buton rock asphalt (BRA) was chosen as the study subject. The thermal stability and aging resistance of asphalt modified by BRA, compound-modified asphalt by BRA/SBR, and compound-modified asphalt by BRA and nano-$CaCO_3$ were determined to identify whether the compound modifiers in the asphalt would have a negative effect on the thermal stability and aging resistance of the asphalt. The dynamic shear rheometer (DSR) test was employed to evaluate the thermal stability. The thin film oven test (TFOT) and pressure aging vessel (PAV) were adopted to determine the aging resistance. The viscoelastic characteristics of asphalt with and without modifiers were revealed to evaluate the low-temperature crack resistance of asphalt modified by compound modifiers. The bending beam rheometer (BBR) creep test was conducted in three test temperatures in order to determine the creep stiffness modulus of the BRA compound-modified asphalt. The viscoelastic model considering the damage caused by loading was established; then, the creep compliance and parameters of the viscoelastic damage model were implemented to evaluate the low-temperature performance of the compound-modified asphalt. The results show that the compound modifiers have little negative effects on the thermal stability and aging resistance of asphalt. The thermal crack resistance of the compound-modified asphalt by BRA/SBR was the best, followed by the compound-modified asphalt by BRA and nano-$CaCO_3$ within the three materials. The accuracy of forecasting the characteristics of compound-modified asphalt was improved by using the viscoelastic model and considering the damage effect.

Keywords: modified asphalt; rock asphalt; creep test; thermal crack; viscoelastic model

1. Introduction

The asphalt pavement structure is widely employed in most high-grade road projects. However, due to the characteristics of the axle load, heavy traffic flow, and traffic channelization of modern highway traffic, the requirements of road materials are constantly improved. The traditional asphalt materials and design methods [1–4] can no longer meet the requirements of the durability of asphalt pavement. Therefore, in order to develop a new type of compound-modified asphalt with excellent thermal stability, low-temperature crack resistance, and good durability, it is necessary to study the performance of modified asphalt.

Buton rock asphalt (BRA) produced from Buton island of South Pacific Indonesia is naturally formed by petroleum or oil continuously emerging from the Earth's crust and impregnating into rocks, followed by evaporation and solidification over millions of years [5,6]. In recent years, BRA has been successfully applied to Chinese road construction for its advantages such as good pavement performance, simple construction technology, et al. There are many studies on Buton rock asphalt. Studies by Wentong Huang have shown that BRA could effectively improve the water stability of the asphalt mixture [7]. Yingmei Yin et al. used dynamic shear rheometer (DSR) to study BRA-modified asphalt that was tested by strain sweep, frequency sweep, and temperature sweep. The results have shown that the rutting factor of the asphalt increased, and the rheological behavior of the asphalt at high temperature was dramatically varied with the increase of the mixing amount of BRA in the asphalt [8]. Ruixia Li et al. tested the chemical composition and structure of BRA-modified asphalt with X-Ray diffraction, infrared spectrum, and thermal analysis. These tests indicated that BRA could effectively improve the adhesion property between asphalt and aggregate [9]. Shaowen Du found that BRA could improve the fatigue resistance of asphalt mixtures [10]. In addition, asphalt mixtures modified by BRA can improve the rutting and skid resistance of asphalt pavement [11,12]. Although BRA has many advantages related to improving the performance of asphalt mixtures and pavement, it can reduce the low-temperature performance of asphalt and asphalt mixtures [13]. The low-temperature performance of BRA-modified asphalt is important, especially in cold regions, so this paper was aimed at finding a modifier to improve the low-temperature of BRA-modified asphalt.

The modification of asphalt binder with polymeric materials and crumb rubber is the most common method to improve the performance of the asphalt binder against most types of distresses [14–17]. Styrene–butadiene rubber (SBR) is widely used as the asphalt modifier for the preparation of polymer-modified asphalt (PMA). SBR is considered to be one of the most effective modifiers for asphalt pavements [18]. The Engineering Brief published [19] on the Federal Aviation Administration website in 1987 described the benefits of SBR-modified asphalt in improving the performance of asphalt concrete pavements and sealant coatings. The low-temperature ductility was improved, the viscosity was increased, the elastic recovery was improved, and the adhesive and cohesive properties were improved. The morphological features of nanomaterials have special features derived from their nanoscale dimensions [20]. Due to the very tiny size and large surface area, the properties of nanomaterials are very different from the normal-sized materials [21]. In recent years, nanomaterials have attracted much attention because of their ability to improve the properties of bituminous materials. Nanotechnology is widely employed in the development of a new generation of materials to improve the macroscopic properties of materials [22,23]. H Raufi et al. studied the performance of nano-$CaCO_3$ modified bitumen in hot mix asphalt; the results showed that an asphalt mixture prepared with 6% nano-$CaCO_3$ modified bitumen exhibited good performances against moisture susceptibility and high-temperature performance [24]. Unique mechanical and rheological properties of nanomaterials are conducive to the design and construction of durable pavement materials [25]. Adding these nanosized particles to another material may overcome the monolithic limitations, and asphalt binders are no exception. The addition of nanomaterials changes the rheological properties of asphalt binders, and may also lead to the changes in the intermolecular forces within the asphalt binder structure [26]. This is because the interaction at the phase interface is greatly increased when the size reaches the nanoscale.

As for evaluation indicators of the low-temperature performance of asphalt, penetration, ductility, equivalent brittle point et al. were adopted widely, but these indicators are empirical and have less relation to the mechanical properties of materials. Therefore, strategic highway research program (SHRP) proposed that the low-temperature performance of asphalt could be evaluated by stiffness modulus obtained by a bending beam rheometer (BBR) creep test, which could set relations between low-temperature performance and mechanical properties [27]. A low-temperature creep test, which tests the property of a material under a constant stress and low temperature, was employed in this paper. In the creep test, the flexibility of material was evaluated by creep compliance, which is the reciprocal of the stiffness modulus. Burgers' model was widely adopted in the studies on the viscoelasticity of asphalt and asphalt mixtures, but it didn't consider the influence of the damage and its distribution. To make Burgers' model conform to the practical test conditions, the Burgers' model coupling the damage was established.

The main objective of this paper is to improve the low-temperature performance of Buton rock asphalt (BRA)-modified asphalt and to establish a characterization method of the low-temperature performance. Two compound modifiers, SBR and nano-$CaCO_3$, were added to the BRA-modified asphalt, respectively. The bending beam rheometer (BBR) creep test was employed under three test temperatures to determine the creep stiffness module of the two compound-modified asphalts. Meanwhile, the amounts of the two mixing modifiers were considered. The viscoelastic model of creep compliance considering the damage effects was proposed.

2. Materials

2.1. Materials

The properties of asphalt binders were measured according to the test methods of specification, the Standard Test Methods of Bitumen and Bituminous Mixtures for Highway Engineering (JTG E20-2011) [28]. AH-70 (penetration grade) base asphalt was used as the binder in this work, and its main technical indicators are summarized in Table 1. The Buton rock asphalt (BRA, Figure 1) that was used in this test had been sifted with an 0.15-mm sieve. The technical indicators of BRA are shown in Table 2. Two kinds of low-temperature modifiers, styrene–butadiene rubber (SBR, Figure 1) and nano-$CaCO_3$ (Figure 1), were adopted in this test. Their main technical properties are presented in Tables 3 and 4, respectively.

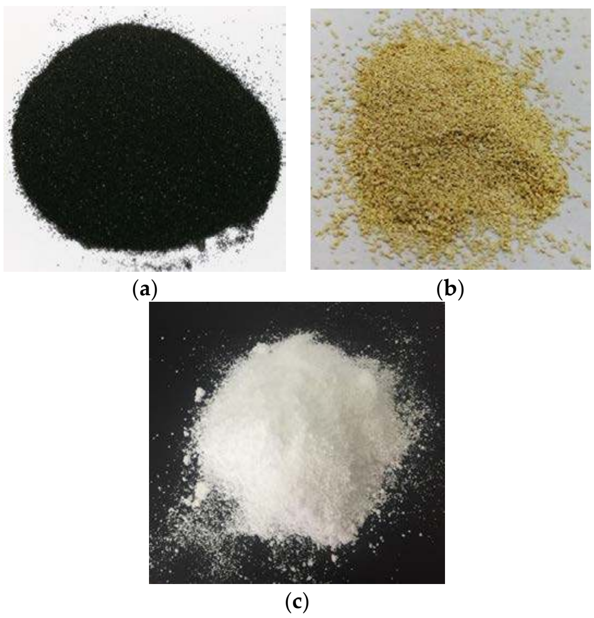

(a) (b) (c)

Figure 1. Materials: (**a**) Buton rock asphalt (BRA); (**b**) styrene–butadiene rubber (SBR); (**c**) Nano-$CaCO_3$.

Table 1. Technical properties of base asphalt binder AH-70.

Test Items	Industry Standard	Test Results	Test Methods [28]
Penetration at 25 °C (0.1 mm)	60	75.2	T 0604-2000
Penetration Index	−2~2	0.968	T 0604-2000
Softening point (°C)	≥100	51.5	T 0606-2000
Ductility at 15 °C (cm)	≥46	>150	T 0605-1993
Rotation viscosity/135 °C (Pa·s)	\	0.451	T 0615-2000

Table 2. Technical properties of BRA.

Test Items		Industry Standard	Test Results	Test Methods [29]
Appearance		Brown powder	Brown powder	JT/T860.5-2014
Ash content (%)		<75	74.14	
Solubility (%)		>25	25.6	
Water content (%)		<2	0.97	
Percentage passing (%)	<4.75 mm	100	100	
	<2.36 mm	90~100	100	
	<0.6 mm	10~60	53	

Table 3. Technical properties of SBR.

Test Items		Industry Standard	Test Results	Test Methods
Volatile matter content (%)		≤0.60	0.30	GB/T 6737
Ash content (%)		≤0.50	0.10	GB/T 4498
Organic acids content (%)		4.50~6.75	6.15	GB/T 8657
Soap content (%)		≤0.50	0.01	
Bound styrene content (%)		22.5~24.5	23.7	GB/T 8658
Raw rubber Mooney viscosity [50 ML(1 + 4)100 °C]		45~55	52	GB/T1232.1
Compound rubber Mooney viscosity [50 ML(1 + 4)100 °C]		≤93	70	
Tensile strength (MPa)		≥25.5	25.8	GB/T 8656 A
Tensile elongation (%)		≥340	412	
300% fixed elongation stress at 145 °C (MPa)	25 min	17.7 ± 2.0	16.6	
	35 min	20.6 ± 2.0	20.8	
	50 min	21.5 ± 2.0	21.6	

Table 4. Technical properties of nano-$CaCO_3$.

Test Items	Test Results	Test Methods [30]
Appearance	White powder	GB/T19590-2011
Nano-$CaCO_3$ content (%)	≥98	
PH value	8.0~10.5	
Whiteness (%)	≥95	
Activation rate (%)	≥98	
Volatile matter content at 105 °C (%)	≤0.5	
Insoluble matter content in hydrochloric acid (%)	≤0.03	
Passing rate for 45-µm experimental sieve (%)	≤0.02	
Oil absorption value (%)	≤35	
Insoluble matter content in hydrochloric acid (%)	≤0.03	
Passing rate for 45-µm experimental sieve (%)	≤0.02	
Oil absorption value (%)	≤35	

2.2. Preparation of Modified Asphalt

Based on the Marshall test results, the determined optimum asphalt content of a base asphalt mixture and BRA-modified mixture of AC-16C were 4.2% and 4.4% by mass of the mixture, respectively. According to the test results and engineering experience, it was determined that the quality content of the BRA was 3% in the BRA-modified asphalt mixture. In the experiment, according to the composition of asphalt and mineral elements (ash) in the BRA, the amount of mineral powder and asphalt was adjusted to ensure that the asphalt content was constant in the BRA-modified asphalt mixture. Based on this, the calculated ratio between the BRA and the base asphalt was 0.83:1. To investigate the effect of the content of SBR and nano-$CaCO_3$ on BRA, BRA with different SBR contents (3%, 5%) and nano-$CaCO_3$ (5%, 10%) contents were prepared, respectively.

Firstly, base asphalt AH-70 was heated to 140 °C. Within the range of 140–145 °C, the asphalt was mixed by a glass rod when it was heated. When the base asphalt melted, the BRA was added into the base asphalt by using the external addition method. Then, the asphalt was kept at 140 °C for 10 min with high-speed shearing equipment running at 4000 rpm. After that, the low-temperature modifiers were respectively added into the asphalt, which having been mixed well, and then, the compounds continued to be mixed for 25–30 min. When all of the processes were finished, the two BRA compound-modified asphalts were prepared. The properties of the modified asphalts were tested, and the results are shown in Table 5.

Table 5. The basic technical properties of modified asphalts.

Test Items	BRA	BRA + 3% SBR	BRA + 5% SBR	BRA + 5% Nano-$CaCO_3$	BRA + 10% Nano-$CaCO_3$
Penetration (25 °C, 0.1 mm)	26.3	24.0	22.4	24.2	22.7
PI	1.862	1.703	1.961	1.870	1.912
$T_{1,2}$ (°C)	−18.8	−16.6	−17.1	−17.7	−17.0
T_{800} (°C)	73.5	73.7	76.5	73.5	74.7
Softening Point (°C)	64.7	75.8	81.4	65.4	66.9
Ductility (5 cm/min, 15 °C, cm)	7.5	20.1	26.7	8.4	12.8

According to the analysis of the basic properties of the compound-modified asphalt in Table 5, it can be concluded that the addition of nano-$CaCO_3$ and SBR can improve the high-temperature stability of the BRA.

To further reveal the impact of the modifier on the performance of the asphalt material, the test of thermal (high and low) performance and aging resistance of BRA compound-modified asphalts was conducted. The thermal stability of the BRA compound-modified asphalt was determined by determining the rheological properties of the asphalt binder using a dynamic shear rheometer. The thermal cracking property characterized by the creep stiffness modulus was tested through using the bending beam rheometer (BBR) test. The creep compliance and parameters of the viscoelastic damage model were implemented to evaluate the low-temperature performance of the compound-modified asphalts. The thin film oven test (TFOT) test was employed to evaluate the short-term aging properties of the compound-modified asphalts and its long-term aging properties were tested by a pressure aging vessel (PAV) test.

3. Tests and Results

3.1. The Evaluation of the Thermal Stability and Aging Resistance for Modified Asphalt

3.1.1. Thermal Stability

The dynamic shear rheometer (DSR) can be employed to measure the rheological properties of asphalt at high and medium temperatures to evaluate the thermal stability of asphalt. Within the viscoelastic range, it was implemented to detect the complex shear modulus G^*, phase angle δ, and anti-rutting factor $G^*/\sin\delta$ of asphalt, and its rheological properties can be evaluated. The test temperature of a dynamic shear rheometer (DSR) starts from 58 °C. If the anti-rutting factor $G^*/\sin\delta$ is qualified, the test was performed at 64 °C for one grade, and the requalification continues to increase to 70 °C for testing until a test temperature of $G^*/\sin\delta < 1.0$ KPa then stopped the test. The complex shear modulus G^* indicates the ability of the material to resist the shear deformation. The greater the value of G^*, the harder the asphalt, which meant a better rutting resistance. The smaller the phase angle was, the more elastic the components in the asphalt.

The dynamic shear rheometer (DSR) test was implemented to qualify the high temperature performance of nano-$CaCO_3$/BRA and SBR/BRA compound-modified asphalt. The results of dynamic shear rheometer (DSR) tests before the aging of nano-$CaCO_3$/BRA and SBR/BRA compound-modified asphalts with different contents are shown in Figures 2–4, respectively.

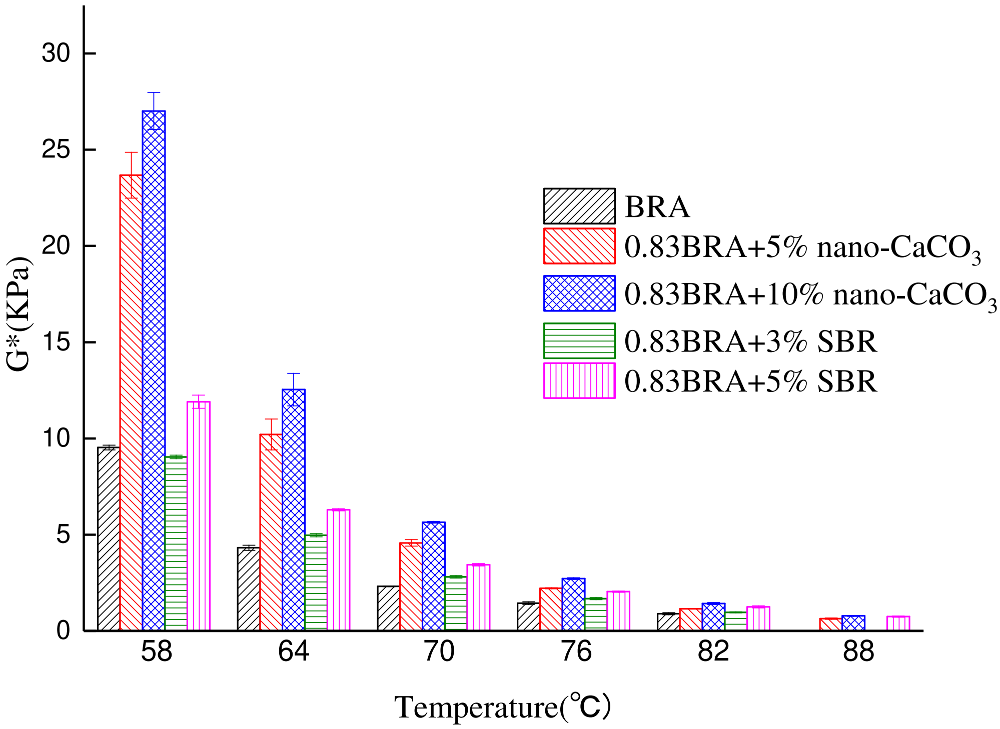

Figure 2. The relationship between complex shear modulus G^* and the temperature of nano-$CaCO_3$/BRA and SBR/BRA compound-modified asphalt.

Figure 2 shows that the complex shear moduli G^* of the five modified asphalts decreasing with increasing temperature. Under the same temperature conditions, the complex shear modulus G^* of 10% nano-$CaCO_3$/BRA compound-modified asphalt is the largest. The BRA has the smallest complex shear modulus G^*. The complex shear modulus of 5% SBR/BRA compound-modified asphalt is much larger than that of 3% SBR/BRA compound-modified asphalt. This shows that the addition of nano-$CaCO_3$ and SBR can significantly improve the resistance of BRA to deformation, and with the increase of the amount of addition, the deformation resistance is enhanced.

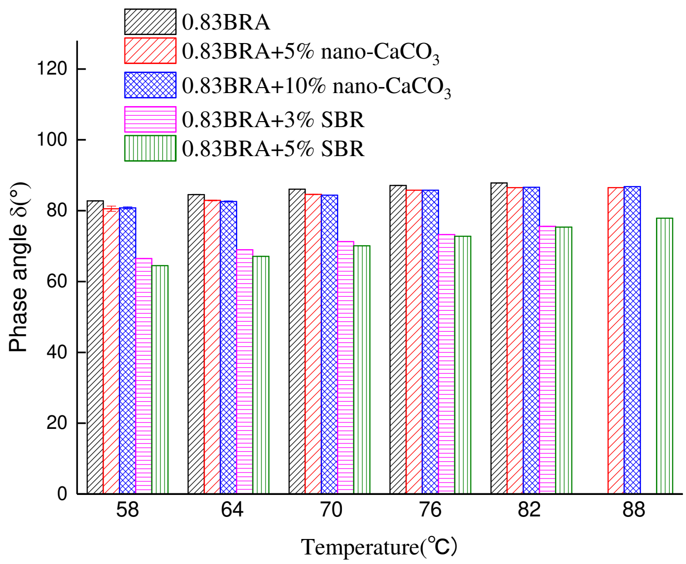

Figure 3. The relationship between phase angle δ and temperature of nano-$CaCO_3$/BRA and SBR/BRA compound-modified asphalt.

As can be observed from Figure 3, under the same temperature conditions, the phase angle δ of the 5% SBR/BRA compound-modified asphalt is the smallest, and that of the BRA is the largest. This shows that the addition of nano-$CaCO_3$ and SBR can improve the elastic composition of the BRA, and the 5% SBR/BRA compound-modified asphalt is the most likely to restore deformation compared with the other four kinds of modified asphalt.

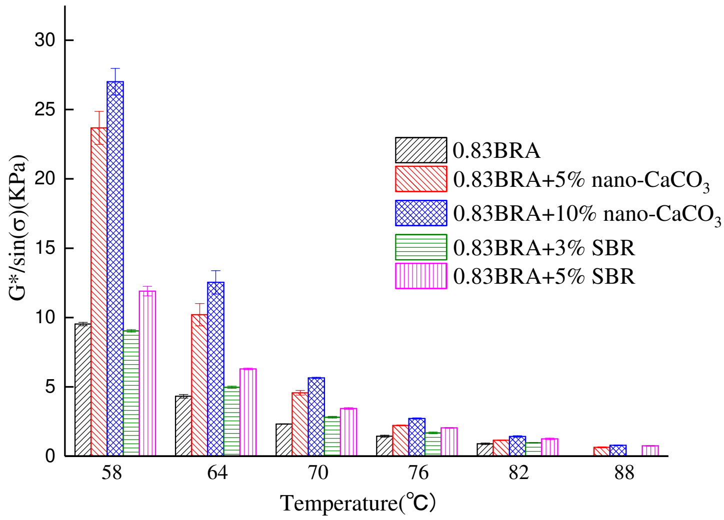

Figure 4. The relationship between anti-rutting factors $G^*/\sin\delta$ and the temperature of nano-$CaCO_3$/BRA and SBR/BRA compound-modified asphalt.

It can be observed from Figure 4 that at the same temperature, the anti-rutting factors $G^*/\sin\delta$ of the four kinds of BRA compound-modified asphalt are larger than that of BRA at the same temperature, and the rutting resistance of 10% nano-$CaCO_3$/BRA compound-modified asphalt is the best. The failure temperature of 10% nano-$CaCO_3$/BRA and 5% SBR/BRA compound-modified asphalts reached 88 °C, which is a temperature grade higher than the failure temperature of 82 °C. It shows that the high temperature properties of nano-$CaCO_3$/BRA, SBR/BRA compound-modified asphalt, and anti-rutting performance are more superior to those of BRA.

3.1.2. Aging Resistance

Asphalt will be aging during the process of storage, mixing, transportation, construction, and service. Due to the long-time contact with air, under the influence of natural conditions, a series of physical and chemical reactions will happen, which will adversely affect the performance of asphalt pavement. The short-term aging of asphalt is mainly caused by the mixing and paving process. There are two test methods for indoor tests to simulate short-term aging: the thin film oven test (TFOT), and the rolling thin film oven test (RTFOT).

(1) Thin Film Oven Test (TFOT) test

The short-term aging test using the thin film oven test (TFOT) was employed in this paper. The stainless steel discs (diameter 140 mm × deep 9.5 mm) were loaded into the ventilation oven. The temperature of the oven was kept at 163 °C and the speed was kept at 5.5 r/min. After 5 h, the weight loss, penetration ratio, and rutting factor [31] of the aged asphalt samples were determined. The changes of indicators for nano-$CaCO_3$/BRA and SBR/BRA compound-modified asphalt after the thin film oven test (TFOT) aging are shown in Table 6.

Table 6. The changes of indicators for nano-$CaCO_3$/BRA and SBR/BRA compound-modified asphalt after thin film oven test (TFOT) aging.

Test Items	BRA	BRA + 3% SBR	BRA + 5% SBR	BRA + 5% Nano-$CaCO_3$	BRA + 10% Nano-$CaCO_3$
Mass loss (%)	0.343	0.279	0.260	0.254	0.229
Penetration (25 °C, 0.1 mm)	26.3	24.0	22.4	24.2	22.7
Penetration of after TFOT aging (0.1 mm)	18.8	22.5	21.4	21.2	20.4
Penetration ratio (%)	70.7	93. 8	95.5	87.6	89.9

From Table 6, it can be observed that the quality of the five modified asphalts has been lost, and the quality loss of the 10% nano-$CaCO_3$/BRA compound-modified asphalt is the least compared to that of the BRA. It shows that, during the aging process, the nano-$CaCO_3$/BRA compound-modified asphalt has relatively less volatilization. The penetration ratio of 5% SBR/BRA compound-modified asphalt is the largest compared to that of BRA, even reaching 95.5%. This indicates that the 5% SBR can significantly improve the anti-aging properties of BRA.

The rutting resistance of the five modified asphalt samples after the thin film oven aging test was compared with rutting resistance before aging. The test data are shown in Figure 5.

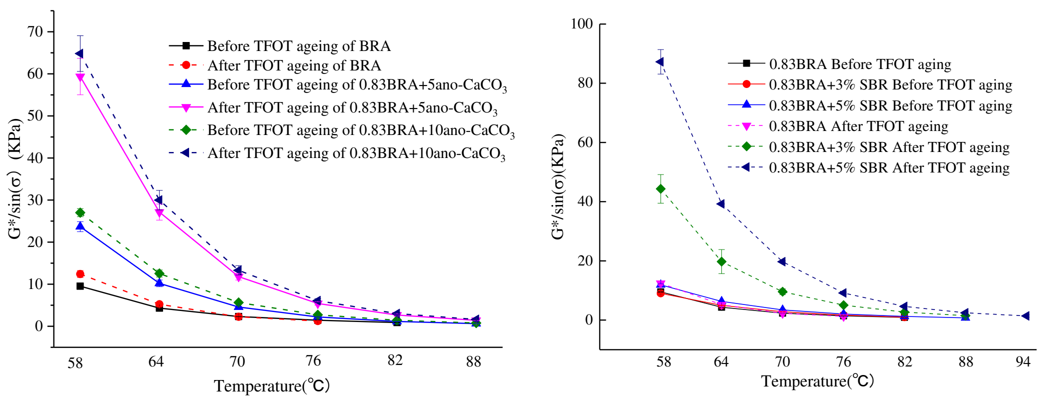

Figure 5. The relationship between Nano-$CaCO_3$/BRA and SBR/BRA compound-modified asphalt in before and after thin film oven test (TFOT) aging anti-rutting factors ($G^*/\sin\delta$) and temperature.

The results can be observed from the curve change in Figure 5. It is known that both the original anti rutting factor and the anti-rutting factor after thin film oven test (TFOT) aging, the nano-$CaCO_3$/BRA, and SBR/BRA compound-modified asphalt are all larger than the BRA. This shows that the addition of SBR and nano-$CaCO_3$ can improve the anti-rutting performance of BRA.

(2) Pressure Aging Vessel (PAV) test

The pressure aging vessel (PAV) aging test is a simulated oxidation aging of asphalt pavement over approximately five to eight years, which is employed to evaluate the antioxidant aging ability of different asphalts under the conditions of temperature and pressure. The test method of pressure aging vessel (PAV) aging is to put a thin film oven test (TFOT) sample into a pressure vessel with a pressure of 2.1 MPa ± 0.1 MPa and temperature of 90~110 °C for 20 h.

The samples of SBR/BRA and nano-$CaCO_3$/BRA compound-modified asphalt with different content were tested with the bending beam rheometer (BBR), and test temperatures of −6 °C and −12 °C were adopted and compared with those before aging. The creep stiffness *S* and the creep slope *m* value of SBR/BRA and nano-$CaCO_3$/BRA compound-modified asphalts were compared before and after pressure aging vessel (PAV) aging, as shown in Figures 6 and 7.

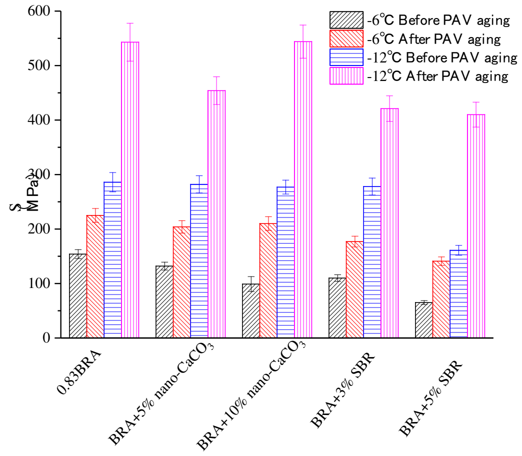

Figure 6. Creep stiffness *S* of nano-$CaCO_3$/BRA and SBR/BRA compound-modified asphalt before and after pressure aging vessel (PAV) aging.

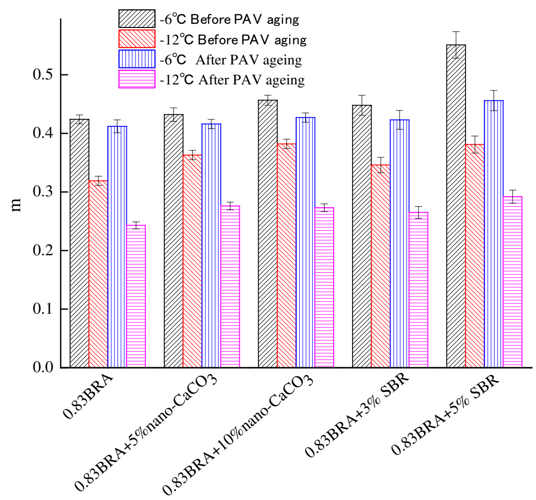

Figure 7. *m* value of nano-$CaCO_3$/BRA and SBR/BRA compound-modified asphalt before and after pressure aging vessel (PAV) aging.

From Figures 6 and 7, it can be observed that at −6 °C, the stiffness S and m value before and after pressure aging vessel (PAV) aging of nano-$CaCO_3$/BRA and SBR/BRA compound-modified asphalt with different contents are satisfied with the requirements of $S \leq 300$ MPa and $m \geq 0.3$. Under the conditions of −6 °C and −12 °C, the S value of the 5% SBR compound-modified asphalt is the smallest relative to the other four kinds of modified asphalt before and after the pressure aging vessel (PAV) aging, but the m value is the largest, compared with the other four kinds of modified asphalt. This indicates that the 5% SBR/BRA compound-modified asphalt has the better low-temperature performance. The reason is that the SBR swells in the asphalt and forms a network structure, which is more resilient and more resistant to deformation.

From Figures 6 and 7, it can be observed that at the different content of nano-$CaCO_3$, the low-temperature performance of BRA slightly improved. This is mainly because the BRA is a porous honeycombed structure, and nano-$CaCO_3$ is a nano-inorganic powder material that can be interspersed in the BRA to better integrate the BRA with the base asphalt. However, nano-$CaCO_3$ is prone to slight agglomeration, which affects the modification effect of base asphalt to some extent.

3.2. The Evaluation of Low-Temperature Performance for Modified Asphalt

3.2.1. Test of Creep Compliance

Strategic highway research program (SHRP) proposed that the low-temperature performance of asphalt can be evaluated by the stiffness modulus obtained by the bending beam rheometer (BBR) creep test, which could build the relationship between the low-temperature performance and mechanical properties [27]. The creep compliance can be employed to characterize the flexibility of the material at low temperature.

The creep compliance is calculated as follows:

$$\sigma_0 = \frac{3PL}{2bh^2} \tag{1}$$

$$\varepsilon(t) = \frac{6h\delta(t)}{L^2} \tag{2}$$

where b is the width of a simply supported beam in mm; h is the height of a simply supported beam in mm; L is the span of a simply supported beam in mm; P is a constant load added on a simply supported beam, P is 100 g × 9.8 N/kg = 0.98 N; $\delta(t)$ is the mid-span deflection of the beam changing with time in mm.

Let Equation (2) divide by Equation (1); then, the creep compliance can be calculated:

$$J(t) = \frac{\varepsilon(t)}{\sigma_0} = \frac{48I}{PL^3}\delta(t) \tag{3}$$

where $J(t)$ is the creep compliance in MPa^{-1}; $\varepsilon(t)$ is the strain of the creep test at different times in mm/mm; σ_0 is the constant stress of creep test in MPa; and I is the moment of inertia for a cross-section of a beam specimen (=$bh^3/12$) in mm^4.

3.2.2. Bending Beam Rheometer Test

The bending beam rheometer (BBR) creep test, according to the controlled stress procedure of ASTM D6648, was conducted [27]. The creep tests of compound-modified asphalt are tested in different test temperatures (−6 °C, −12 °C, and −18 °C) by Thermoelectric bending beam rheometer (TE-BBR) (Figure 8), respectively. The load and deformation in the testing process were automatically collected by a computer data acquisition system.

Figure 8. Thermoelectric bending beam rheometer (BBR) and specimen: (**a**) metal die of BBR; (**b**) asphalt beam of BBR; (**c**) thermoelectric bending beam rheometer.

3.2.3. Results of Creep Test

The curves of creep compliance of BRA compound-modified asphalt in −6 °C, −12 °C, and −18 °C are shown in Figure 9. From analyzing the creep compliance in Figure 9, conclusions can be drawn as below:

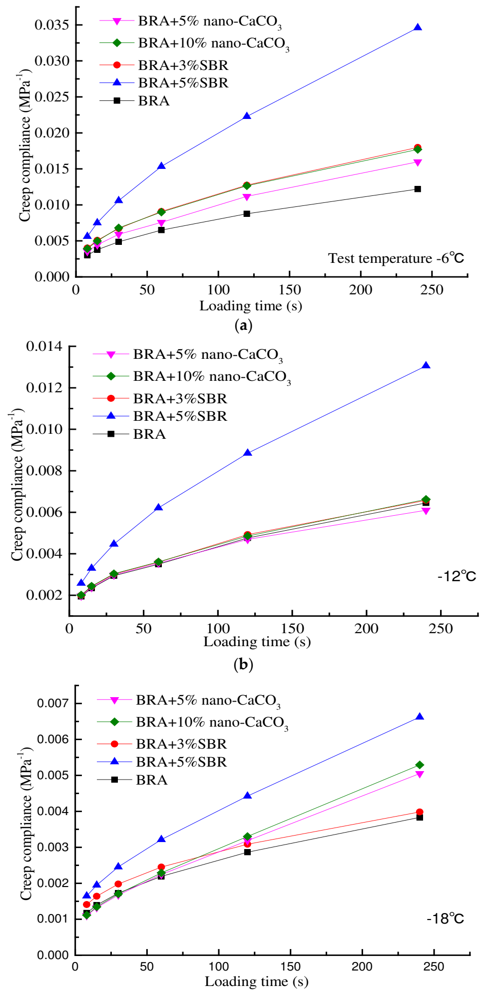

Figure 9. Creep compliance curve of different compound-modified asphalts: (**a**) the curves of creep compliance of BRA compound-modified asphalt in −6 °C; (**b**) the curves of creep compliance of BRA compound-modified asphalt in −12 °C; (**c**) the curves of creep compliance of BRA compound-modified asphalt in −18°C.

(1) Comparison under the same temperature

(a) With the increase of the amounts of SBR, the creep compliance of BRA/SBR compound-modified asphalt will be increased, which means that SBR can improve the flexibility of BRA-modified asphalt. So, the low-temperature performance of BRA-modified asphalt can be improved.

(b) The creep compliance of BRA/nano-$CaCO_3$ compound-modified asphalt slightly increased with an increase of the mixing amount of nano-$CaCO_3$ at the same temperature, which means that the low-temperature performance of BRA/nano-$CaCO_3$ compound-modified asphalt slightly improved. Moreover, the improving effect of nano-$CaCO_3$ on the low-temperature performance of BRA-modified asphalt was less obvious when the temperature was lower.

(2) Comparison under same time

(a) When the temperature was lowered, the compliance of two kinds of BRA compound-modified asphalt decreased, and the modified asphalt hardened.

(b) The creep compliance of BRA/SBR polymer compound-modified asphalt was larger than BRA-modified asphalt.

(c) As the temperature decreased, the creep compliance of BRA/nano-$CaCO_3$ compound-modified asphalt was close to that of BRA. It means that the improving effect of nano-$CaCO_3$ on the low-temperature performance of BRA-modified asphalt was not obvious.

In conclusion, BRA/SBR polymer compound-modified asphalt containing 5% SBR had the greatest creep compliance compared with the other asphalts in the same temperature and the same test time. So, SBR can improve the low-temperature performance of BRA-modified asphalt, and its suitable content is 5% in BRA-modified asphalt.

4. Viscoelastic Damage Model Considering the Damage Effect

4.1. The Establishment of Viscoelastic Damage Model Considering the Damage

To obtain the viscoelastic characteristics for asphalt, Burgers' model was used in many research studies. Lots of studies have demonstrated that asphalt is a viscoelastic fluid material, so asphalt's elasticity, viscoelasticity and flow limitation should be considered when the mechanical characteristics of asphalt are analyzed. Burgers' model is a viscoelastic model that is suitable for analyzing asphalt's rheological behavior. Burgers' model is made up of the Maxwell model and the Kelvin model, and is successfully applied to the viscoelastic analysis of asphalt and asphalt mixtures [32–35].

Burgers' model is shown in Figure 10.

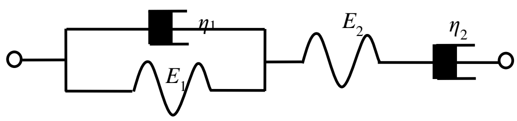

Figure 10. Burgers' model.

The expression for the creep compliance of Burgers' model is given by:

$$J(t) = \frac{1}{E_1} + \frac{t}{\eta_1} + \frac{1}{E_2}\left[1 - \exp\left(-\frac{t}{\tau}\right)\right] \quad (4)$$

where $\tau = \eta_2/E_2$; E_1, η_1, E_2 and η_2 are the viscoelastic parameters of Burgers' model.

However, from the point of view of the mechanics of damage, if asphalt is under a constant load in the bending creep test, lots of microdefects in the materials will occur [36]. Therefore, if the prediction of creep compliance is under the consideration of the damage factor in a special test temperature, the actual values and the fitted values have a very high fitting precision.

It is known from the formation and distribution of material defects that the defects are discrete in the material. However, in the need of research, continuum damage mechanics make material defects continuous, and use damage variables to characterize the effect of defects on the material. Many studies suggest that the Weibull distribution is suitable for the characterization of the defects distribution within a material, and has been widely used to analyze the fatigue damage characterization of asphalt and asphalt mixtures [37–41]. If microdefects in BRA compound-modified asphalt obey the Weibull distribution, the microdefects' density function changing with time is under:

$$f(t) = \frac{m}{n}(t-\gamma)^{m-1}\exp\left[-\frac{(t-\gamma)^m}{n}\right] \tag{5}$$

where m and n are the material parameters obtained by the regression of data of experiments.

$$\frac{dD(t)}{dt} = f(t) \tag{6}$$

The results of integrating Equations (2) and (3) are calculated as follows:

$$D(t) - D(\gamma) = \int_{\gamma}^{t}\frac{m}{n}(x-\gamma)^{m-1}\exp\left[-\frac{(x-\gamma)^m}{n}\right]dx \tag{7}$$

If the initial damage factor $D(\gamma)$ = 0, Equation (7) is simplified as:

$$D(t) = 1 - \exp\left[-\frac{(t-\gamma)^m}{n}\right] \tag{8}$$

where γ = critical time of defects starting to form, γ is considered as 0 in the test, and then the continuous damage factor is simplified as:

$$D(t) = 1 - \exp\left(-\frac{t^m}{n}\right) \tag{9}$$

$$\begin{aligned}\varepsilon(t) = & \ [1-D(t)]^{-1}\sigma_0 J(t) \\ & = \exp\left(\tfrac{t^m}{n}\right)\sigma_0\left\{\tfrac{1}{E_1} + \tfrac{t}{\eta_1} + \tfrac{1}{E_2}\left[1-\exp\left(-\tfrac{t}{\tau}\right)\right]\right\}\end{aligned} \tag{10}$$

From Equation (9), the existence of defects increases the creep strain's growth. Thus, if the damage is considered, the model for the variation of creep compliance of viscoelastic material will be accurate.

After putting σ_0 to the left of Equation (10), Burgers' constitutive mode considering defects in material is given by:

$$\begin{aligned}J'(t) & = \tfrac{\varepsilon(t)}{\sigma_0} \\ & = \exp\left(\tfrac{t^m}{n}\right)\left\{\tfrac{1}{E_1} + \tfrac{t}{\eta_1} + \tfrac{1}{E_2}\left[1-\exp\left(-\tfrac{t}{\tau}\right)\right]\right\}\end{aligned} \tag{11}$$

4.2. Fitting Results of Viscoelastic Damage Model

The viscoelastic properties of two kinds of BRA compound-modified asphalt are analyzed by the viscoelastic damage model established in this paper. This Levenberg–Marquardt method was implemented to fit the creep compliance of BRA-modified asphalt in −6 °C, −12 °C, and −18 °C. The parameters of creep compliance of the viscoelastic damage model are shown in Table 7. The columnar diagram viscoelastic parameters (E_1, E_2, η_1 and η_2) of the model changed with temperature are shown in Figure 11.

Table 7. Fitting results of viscoelastic damage model and Burgers' model for different asphalts.

T (°C)	Asphalt Type	*m*	*n*	E_1 (MPa)	E_2 (MPa)	η_1 (MPa·s)	η_2 (MPa·s)	τ (s)	R^2
−6	BRA	0.123	321.869	546.8	302.0	33,912.3	8225.6	27.24	0.9989
	+3% SBR	0.100	442.900	423.1	209.7	21,979.7	6223.6	29.68	0.9990
	+5% SBR	0.010	2634.839	357.9	127.0	9948.6	3930.3	30.95	0.9994
	+5% nano-$CaCO_3$	0.093	452.713	446.0	277.2	23,538.8	8207.3	29.61	0.9985
	+10% nano-$CaCO_3$	0.086	513.592	480.0	182.9	22,868.5	5118.1	27.98	0.9988
−12	BRA	0.159	321.821	717.6	680.1	66,678.5	16,874.3	24.81	0.9983
	+3% SBR	0.168	275.811	706.5	631.0	66,919.3	16,043.5	25.43	0.9979
	+5% SBR	0.066	854.2	684.2	326.3	27,941.3	9520.7	29.18	0.9993
	+5% nano-$CaCO_3$	0.190	167.516	759.9	590.2	78,495.5	13,824.1	23.42	0.9976
	+10% nano-$CaCO_3$	0.152	392.156	691.7	678.2	64,479.4	15,774.8	23.26	0.9985
−18	BRA	0.215	192.268	1220.6	998.7	121,513.3	27,984.9	28.02	0.9988
	+3% SBR	0.272	142.491	981.0	937.4	132,872.4	24,969.3	26.64	0.9985
	+5% SBR	0.148	1955.665	790.8	966.2	55,410.8	30,105.7	31.159	0.9999
	+5% nano-$CaCO_3$	−20.539	0.005	1150.8	1848.8	65,875.3	55,528.0	30.03	0.9999
	+10% nano-$CaCO_3$	−10.058	0.431	1128.3	1975.7	61,545.1	59,415.5	30.07	0.9999

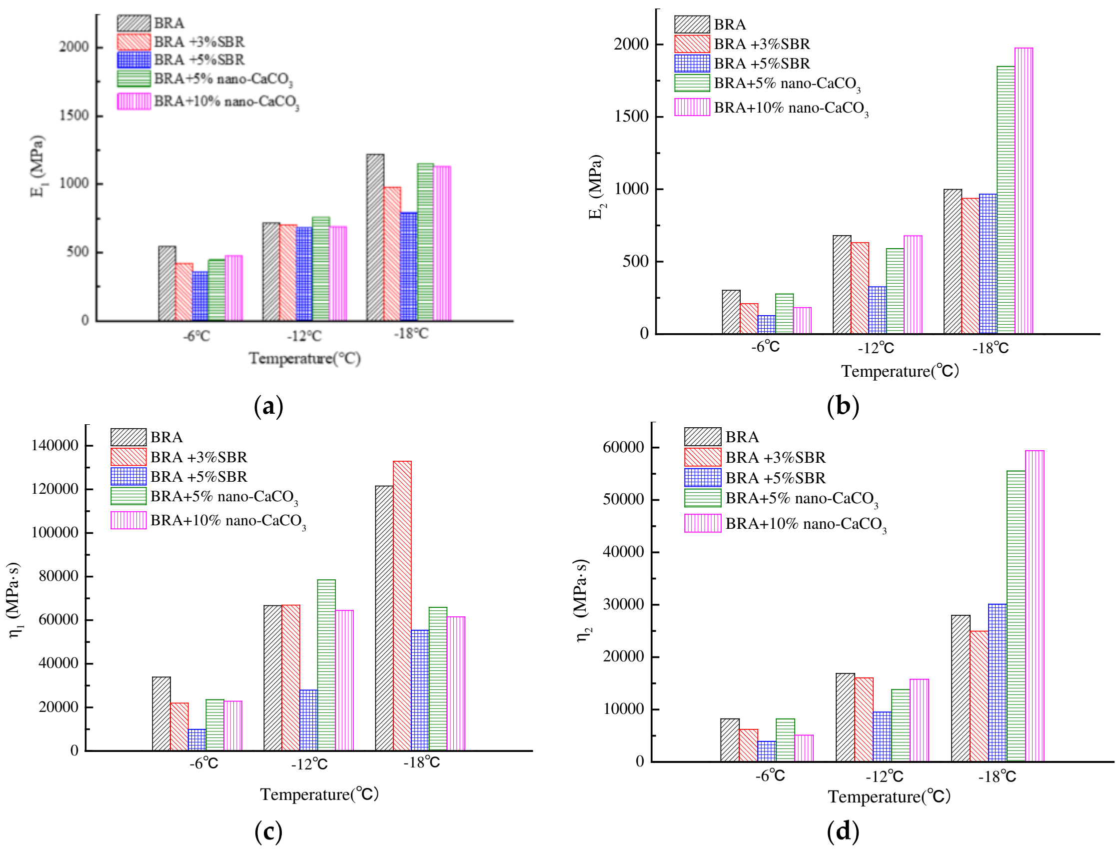

Figure 11. The comparison among viscoelastic damage model's parameters of creep compliance: (**a**) the viscoelastic parameters (E_1) of the model changed with temperature; (**b**) the viscoelastic parameters (E_2) of the model changed with temperature; (**c**) the viscoelastic parameters (η_1) of the model changed with temperature; (**d**) the viscoelastic parameters (η_2) of the model changed with temperature.

(a) The coefficient of determination R^2 between the model and test data shown in Table 7 indicated that the fitting degree of test data and creep compliance of viscoelastic damage model is very precise. So, considering the effect of microdefects during the loading process can improve the precision in the prediction of viscoelastic parameters of compound-modified asphalt.

(b) As shown in Figure 11a,b,d, the viscoelastic parameters (E_1, E_2 and η_2) of BRA compound-modified asphalt increased as the temperature decreased, which indicated that the low-temperature performance of the material decreased. Among the viscoelastic parameters, E_2 and η_2 had the same change trend as the temperature decreased, so both have good correlation with each other.

(c) In three test temperatures, the viscoelastic parameters (E_1, E_2, and η_1) of BRA compound-modified asphalt, in which 5% SBR was the smallest among the test conditions, indicated that SBR could improve the flexibility and low-temperature performance of BRA-modified asphalt. The difference of viscoelastic parameters between BRA/nano-$CaCO_3$ compound-modified and BRA-modified asphalt is not obvious, which indicated that nano-$CaCO_3$ couldn't effectively improve the low-temperature performance of BRA-modified asphalt.

In conclusion, SBR can reduce the parameter values of BRA-modified asphalt and improve its flexibility effectively at low temperature. In order to improve the low-temperature performance, it is effective to add SBR into BRA-modified asphalt.

In this paper, the low-temperature performance of BRA compound-modified asphalt was evaluated only through asphalt, whereas the performance of an asphalt mixture is even closer to asphalt pavement than asphalt itself. So, subsequent research should focus on the performance of a SBR/BRA compound-modified asphalt mixture.

5. Conclusions

According to test and analysis results, the following conclusions were drawn:

1. The suitable addition of nano-$CaCO_3$ and SBR can improve the thermal stability and without negative effects to the aging resistance of BRA-modified asphalt to some extent. The anti-rutting performance of 10% BRA/nano-$CaCO_3$ compound-modified asphalt was the best. The thermal cracking performance of 5% BRA/SBR-modified asphalt has been effectively improved, and that of nano-$CaCO_3$ is not obvious.
2. The prediction accuracy of the viscoelasticity for compound-modified asphalt has been raised by the improved Burgers' model, and considered the effect of damage. The creep compliance shows a good agreement with the experimental results, so it can be applied to analyze the viscoelasticity of compound-modified asphalt.
3. The viscoelastic parameters (E_1, E_2 and η_1) of BRA compound-modified asphalt increased with the decrease of temperature, which indicated that the flexibility of the material decreased.

Author Contributions: Data curation, S.L., S.W. and C.X.; Formal analysis, S.L., S.W. and C.X.; Funding acquisition, S.L., T.G. and G.H.; Investigaton, S.L.; Methodology, S.L.; Project administration, S.L.; Resources, S.L.; Supervision, S.L.; Visualization, S.L.; Writing—original draft, S.L., S.W., T.G., C.X. and J.L.; Writing—review & editing, S.L. and C.X.

Funding: This research was funded by National Natural Science Foundation of China (Grant number [51578081, 51608058]; The Ministry of Transport Construction Projects of Science and Technology [2015318825120]; The Guangxi Zhuang Autonomous Region Traffic and Transportation Department Transportation Projects of Science and Technology [2013-32], and The Inner Mongolia Autonomous Region Traffic and Transportation Department Transportation Projects of Science and Technology [NJ-2016-35].

Acknowledgments: This work is supported by Key Projects of Hunan Province-Technological Innovation Project in Industry [2016GK2096], National Engineering Laboratory Open Fund Project [kfh160102], Scientific and Technological Innovation Project of Hunan Province for University Graduate Students [CX2017B457]. The authors gratefully acknowledge their financial support.

Conflicts of Interest: The authors declare no conflict of interest.

References

1. Lv, S.; Liu, C.; Yao, H.; Zheng, J. Comparisons of synchronous measurement methods on various moduli of asphalt mixtures. *Constr. Build. Mater.* **2018**, *158*, 1035–1045. [CrossRef]
2. Lv, S.; Liu, C.; Chen, D.; Zheng, J.; You, Z.; You, L. Normalization of fatigue characteristics for asphalt mixtures under different stress states. *Constr. Build. Mater.* **2018**, *177*, 33–42. [CrossRef]

3. Zhang, C.; Wang, H.; You, Z.; Liu, Y.; Yang, X.; Xiao, J. Prediction on rutting decay curves for asphalt pavement based on the pavement-ME and matter element analysis. *Int. J. Pavement Res. Technol.* **2017**, *10*, 466–475. [CrossRef]
4. Lv, S.; Fan, X.; Xia, C.; Zheng, J.; Chen, D.; You, L. Characteristics of Moduli Decay for the Asphalt Mixture under Different Loading Conditions. *Appl. Sci.* **2018**, *8*, 840. [CrossRef]
5. Li, R.; Karki, P.; Hao, P.; Bhasin, A. Rheological and low temperature properties of asphalt composites containing rock asphalts. *Constr. Build. Mater.* **2015**, *96*, 47–54. [CrossRef]
6. Lv, S.; Wang, X.; Liu, C.; Wang, S. Fatigue Damage Characteristics Considering the Difference of Tensile-Compression Modulus for Asphalt Mixture. *J. Test. Eval.* **2018**, *46*, 20170114. [CrossRef]
7. Huang, W. Experimental Investigation into Pavement Performance of Buton Rock Asphalt Mixtures. *J. South China Univ. Technol.* **2012**, *208*, 122–135. [CrossRef]
8. Yin, Y.M.; Zhang, X.N. Research on high temperature rheological characteristics of asphalt mastics with indonesian buton rock asphalt (BRA). *J. Wuhan Univ. Technol.* **2010**, *32*, 85–89. [CrossRef]
9. Ruixia, L.I.; Hao, P.; Wang, C.; Zhang, Q. Modified Mechanism of Buton Rock Asphalt. *J. Highw. Transp. Res. Dev.* **2011**, *12*, 4.
10. Du, S.W. Performance and mechanism of BRA-SBS polymer composite modified asphalt mixture. *J. Build. Mater.* **2012**, *15*, 871–874.
11. Hadiwardoyo, S.P.; Sinaga, E.S.; Fikri, H. The influence of Buton asphalt additive on skid resistance based on penetration index and temperature. *Constr. Build. Mater.* **2013**, *42*, 5–10. [CrossRef]
12. Wang, H.B.; Zhe-Sheng, G.E. Test of Dynamic Rheology Properties of Buton Rock Asphalt Modified Asphalt Cement at High-temperature. *J. Highw. Transp. Res. Dev.* **2008**, *9*, 25.
13. Kocevski, S.; Yagneswaran, S.; Xiao, F.; Punith, V.S.; Smith, D.W.; Amirkhanian, S. Surface modified ground rubber tire by grafting acrylic acid for paving applications. *Constr. Build. Mater.* **2012**, *34*, 83–90. [CrossRef]
14. Wang, M.; Lin, F.; Liu, L. Dynamic Rheological Properties and Microscopic Characteristics of Ash Mastics. *J. Tongji Univ.* **2016**, *44*, 567–571.
15. Nazari, H.; Naderi, K.; Moghadas Nejad, F. Improving aging resistance and fatigue performance of asphalt binders using inorganic nanoparticles. *Constr. Build. Mater.* **2018**, *170*, 591–602. [CrossRef]
16. Zhang, F.; Hu, C. The research for SBS and SBR compound modified asphalts with polyphosphoric acid and sulfur. *Constr. Build. Mater.* **2013**, *43*, 461–468. [CrossRef]
17. You, Z.; Orcid, Q.D.; Xiao, F. Advanced Paving Materials and Technologies. *Appl. Sci.* **2018**, *8*, 588. [CrossRef]
18. Yildirim, Y. Polymer modified asphalt binders. *Constr. Build. Mater.* **2007**, *21*, 66–72. [CrossRef]
19. Fang, C.; Yu, R.; Liu, S.; Li, Y. Nanomaterials Applied in Asphalt Modification: A Review. *J. Mater. Sci. Technol.* **2013**, *29*, 589–594. [CrossRef]
20. Yao, H.; You, Z.; Li, L.; Goh, S.W.; Lee, C.H.; Yap, Y.K.; Shi, X. Rheological properties and chemical analysis of nanoclay and carbon microfiber modified asphalt with Fourier transform infrared spectroscopy. *Constr. Build. Mater.* **2013**, *38*, 327–337. [CrossRef]
21. Jamshidi, A.; Mohd Hasan, M.R.; Yao, H.; You, Z.; Hamzah, M.O. Characterization of the rate of change of rheological properties of nano-modified asphalt. *Constr. Build. Mater.* **2015**, *98*, 437–446. [CrossRef]
22. Li, R.; Xiao, F.; Amirkhanian, S.; You, Z.; Huang, J. Developments of nano materials and technologies on asphalt materials—A review. *Constr. Build. Mater.* **2017**, *143*, 633–648. [CrossRef]
23. Jahromi, S.G.; Khodaii, A. Effects of nanoclay on rheological properties of bitumen binder. *Constr. Build. Mater.* **2009**, *23*, 2894–2904. [CrossRef]
24. Raufi, H.; Topal, A.; Kaya, D.; Sengoz, B. Performance Evaluation of Nano-$CaCO_3$ Modified Bitumen in Hot Mix Asphalt. In Proceedings of the 18th IRF World Road Meeting, Delhi, India, 14–17 November 2017.
25. Jamal Khattak, M.; Khattab, A.; Rizvi, H.R. Characterization of carbon nano-fiber modified hot mix asphalt mixtures. *Constr. Build. Mater.* **2013**, *40*, 738–745. [CrossRef]
26. Guo, N.; You, Z.; Tan, Y.; Zhao, Y. Performance evaluation of warm mix asphalt containing reclaimed asphalt mixtures. *Int. J. Pavement Eng.* **2016**, *18*, 1–9. [CrossRef]
27. ASTM. *Standard Test Method for Determining the Flexural Creep Stiffness of Asphalt Binder Using the Bending Beam Rheometer (BBR)*; ASTM: West Conshohocken, PA, USA, 2008.
28. Renmin Communication Press. *Specifications and Test Methods of Bitumen and Biminous Mixtures for Highway Engineering*; JTG E20-2011; Renmin Communication Press: Beijing, China, 2011.

29. Renmin Communication Press. *Modifier for Asphalt Mixture Part 5: Natural Asphalt*; JT/T860.5-2014; Renmin Communication Press: Beijing, China, 2014.
30. Renmin Communication Press. *Nanoscale Calcium Carbonate (Powdered Form)*; GB/T19590-2011; Renmin Communication Press: Beijing, China, 2011.
31. Chen, H.; Yan, Z.; Wang, B. Dynamic mechanics performance of aged SBS modified-asphalt. *J. Changan Univ.* **2009**, *29*, 1–5.
32. Liang, H.; Ling, T.; Yu, M.; Zhao, Y.; Tao, M.; Huang, X. High-temperature creep properties of asphalt-rubber and mixture with Sasobit warm mix additives. *J. Changan Univ.* **2015**, *35*, 16–23.
33. Hossain, M.I.; Faisal, H.M.; Tarefder, R.A. Characterisation and modelling of vapour-conditioned asphalt binders using nanoindentation. *Int. J. Pavement Eng.* **2015**, *16*, 382–396. [CrossRef]
34. Gao, D.Y.; Huang, C.S. Viscoelastic Mechanical Model with Five Units and Eight Parameters for Fiber Reinforced Asphalt Concrete. *China J. Highw. Trans.* **2014**, *27*, 1–8, 34.
35. Arabani, M.; Kamboozia, N. The linear visco-elastic behaviour of glasphalt mixture under dynamic loading conditions. *Constr. Build. Mater.* **2013**, *41*, 594–601. [CrossRef]
36. Tsinghua University Press. *Damage Mechanics*; Tsinghua University Press: Beijing, China, 1997.
37. Sharma, H.; Swamy, A.K. Development of probabilistic fatigue curve for asphalt concrete based on viscoelastic continuum damage mechanics. *Int. J. Pavement Res. Technol.* **2016**, *9*, 270–279. [CrossRef]
38. Yi, J.; Shen, S.; Muhunthan, B.; Feng, D. Viscoelastic–plastic damage model for porous asphalt mixtures: Application to uniaxial compression and freeze–thaw damage. *Mech. Mater.* **2014**, *70*, 67–75. [CrossRef]
39. Qian, Z.D.; Wang, J.Y.; Wang, Y.Q. Fatigue Performance of Composite Structure for Perpetual Pavement on Cement Concrete Bridge Deck. *China J. Highw. Trans.* **2012**, *25*, 67–73.
40. Zheng, J.; Lv, S.; Tian, X. Viscoelastic Damage Characteristics of Asphalt Based on Creep Test. *Eng. Mech.* **2008**, *25*, 193–196.
41. Falchetto, A.C.; Moon, K.H. Simple Approach to the Investigation of Asphalt Mixture Strength on Small Beam Specimens at Low Temperature. *J. Mater. Civ. Eng.* **2016**, *29*, 1–11. [CrossRef]